Proceedings of the 15th International Conference on the Application of Accelerators in Research and Industry, J.L. Duggan and I.L. Morgan (eds.), American Institute of Physics Conference Proceedings **475**, p. 541 (1999)

SIMNRA, a Simulation Program for the Analysis of NRA, RBS and ERDA

M. Mayer

Max-Planck-Institut für Plasmaphysik, D-85748 Garching, Germany

SIMNRA is a Microsoft Windows 95/Windows NT program with fully graphical user interface for the simulation of non-Rutherford backscattering, nuclear reaction analysis and elastic recoil detection analysis with MeV ions. About 300 different non-Rutherford and nuclear reactions cross-sections are included. SIMNRA can calculate any ion-target combination including incident heavy ions and any geometry including transmission geometry. Arbitrary multi-layered foils in front of the detector can be used. Energy loss straggling includes the corrections by Chu to Bohr's straggling theory, propagation of straggling in thick layers, geometrical straggling and straggling due to multiple small angle scattering. The effects of plural large angle scattering can be calculated approximately. Typical computing times are in the range of several seconds.

INTRODUCTION

Rutherford backscattering spectroscopy (RBS), nuclear reaction analysis (NRA) and elastic recoil detection analysis (ERDA) with MeV ions are powerful tools for the analysis of the near surface layers of solids. During the last decade several computer programs for the simulation and analysis of spectra obtained in MeV ion beam analysis were developed [1], such as the widely used RUMP [2]. The increase in computer power during the last years has made it possible to drop several limitations of previous programs, which were necessary due to computing time limitations. Additionally an error tolerant fully graphical user interface (GUI) for easy use of the program is highly wishful.

This paper describes the physics concepts of the program SIMNRA (version 4.4). More details can be found in [3, 4].

BASIC CONCEPT

The solid is bombarded by ions with energy E_0. For spectrum synthesis the solid is divided into shallow sublayers with thickness Δx. The simulated spectrum is made up of the superimposed contributions of each reaction[1] from each isotope of each element of each sublayer of the solid. This is illustrated schematically in Fig. 1. The energy spectrum of one reaction of a sublayer is called a "brick" [2]. The brick area is determined from the mean reaction cross-section in the sublayer, while its shape (i.e. the heights of the front and back edges) is determined from the cross-sections at the entrance and exit of the sublayer and the change of the stopping power. The brick has to be folded with the different energy spread contributions, which vary from the front to the backside of the brick, see Fig. 1. To calculate the content of each channel the folded spectrum has to be integrated over a channel width, which is evaluated exactly using Gauss-Legendre integration.

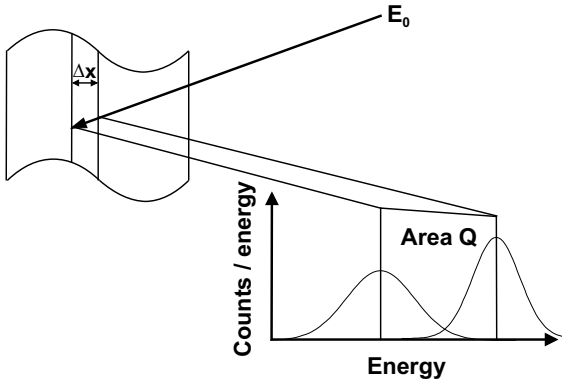

FIGURE 1. Schematic representation of the "brick" concept.

The step width Δx is the most crucial parameter both for the accuracy of the simulation and computing speed. By default SIMNRA uses automatic step width control: The step size Δx is chosen in such a way that the width of the brick is about equal to the full width at half maximum (FWHM) of the energy spread, resulting in small step widths near the surface and larger step widths deep inside the solid, where the depth resolution becomes poor.

CROSS-SECTION DATA

The scattering of two charges is described by the differential Rutherford cross-section, which can be found in many text books, see for example [5]. However, ac-

[1] A reaction may be, generally, scattering of the projectile ion, creation of a recoil or a nuclear reaction.

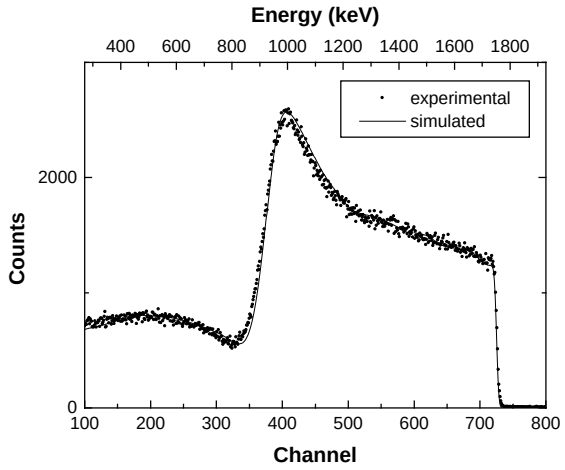

FIGURE 2. Backscattering of 2000 keV protons from silicon, scattering angle $\theta = 165°$. Dots: experimental data; solid line: calculation with SIMNRA, cross-section data from [11].

tual cross-sections deviate from the Rutherford cross-section at both high and low energies for all projectile-target pairs.

The low-energy departures are caused by partial screening of the nuclear charges by the electron shells surrounding both nuclei [5, 6]. This screening is taken into account by a correction factor $F(E, \theta)$. SIMNRA uses the angular- and energy dependent correction factor from [6] both for scattered particles and recoils.

At high energies the cross-sections deviate from the Rutherford cross-section due to the influence of the nuclear force [7], and empirical cross-section data have to be used. About 300 different experimental cross-section data sets for non-Rutherford scattering and nuclear reactions for incident protons, deuterons, ^{3}He and ^{4}He ions are included with SIMNRA. Most of the cross-section data were collected by Foster *et al.* [8] and Cox *et al.* [9], they are available at SigmaBase [10]. Some additional cross-section data sets were added by the author. SIMNRA can use differential and total cross-section data. New cross-section data can be added easily by the user.

As an example for the use of non-Rutherford scattering cross-sections Fig. 2 shows the measured and simulated spectra of 2000 keV protons backscattered from silicon.

STOPPING POWER DATA

SIMNRA can use two different sets of electronic stopping power data: The Andersen-Ziegler data for hydrogen and helium ions from [12, 13] and the more recent stopping power data by Ziegler, Biersack and Littmark from [14]. The electronic stopping power of heavy ions in all elements is derived from the stopping power of protons using Brandt-Kitagawa theory [14, 15], the formalism is described in detail in [14].

The nuclear stopping power for helium and heavy ions is calculated with the universal ZBL potential from [14]. The nuclear stopping component for hydrogen isotopes is very small and is neglected.

Stopping in Compounds

SIMNRA uses Bragg's rule [16] for the determination of the stopping power in compounds. However, Bragg's rule assumes that the interaction between the ion and a target atom is independent of the environment. The chemical and physical state of the medium is, however, observed to have an effect on the energy loss, resulting in deviations from Bragg's rule which are most pronounced around the stopping power maximum and for solid compounds such as oxides, nitrides and hydrocarbons. The deviations from Bragg's rule predictions may be of the order of 10–20% [15]. To account for deviations from Bragg's rule SIMNRA offers the option to multiply the stopping power of each layer with a constant correction factor for each ion species.

ENERGY STRAGGLING

Energy Loss Straggling

When a beam of charged particles penetrates matter, the slowing down is accompanied by a spread of the beam energy which is due to statistical fluctuations of the energy transfer in the collision processes. For thin layers and small energy losses the energy distribution is non-Gaussian and asymmetric [17]. This regime is not implemented in SIMNRA. As the number of collisions becomes large, the distribution of particle energies becomes Gaussian. This regime is described by Bohr's theory [18, 19]. However, Bohr's theory of electronic energy loss straggling is only valid in the limit of high ion velocities. For lower ion energies the deviations caused by the electron binding in the target atoms have to be taken into account. Chu [19, 20] has calculated a correction factor H by using the Hartree-Fock-Slater charge distribution to obtain more realistic values for the electronic energy loss straggling. Graphical representations of H for all elements and various energies can be found in [19, 21]. For low energies and high target Z the Chu straggling theory yields considerably smaller values than the original Bohr theory, for high energies H approaches unity.

For the nuclear energy loss straggling SIMNRA uses Bohr's theory of nuclear straggling [17]. Electronic and nuclear energy loss straggling are independent and are added quadratically.

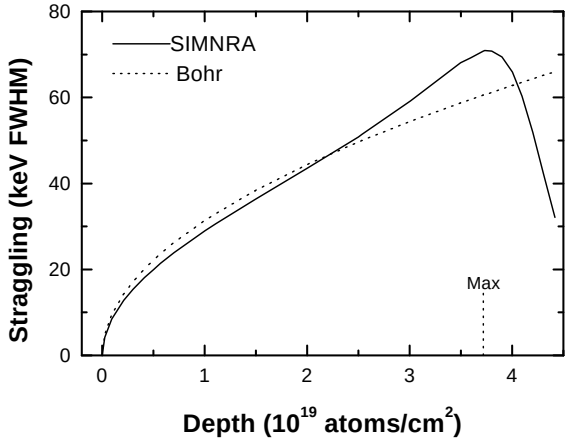

FIGURE 3. Energy loss straggling (FWHM) of 2500 keV ^{4}He ions in Si. Solid line: SIMNRA; dashed line: Bohr's theory. Max: depth at which the particles energy has decreased to the energy of the stopping power maximum.

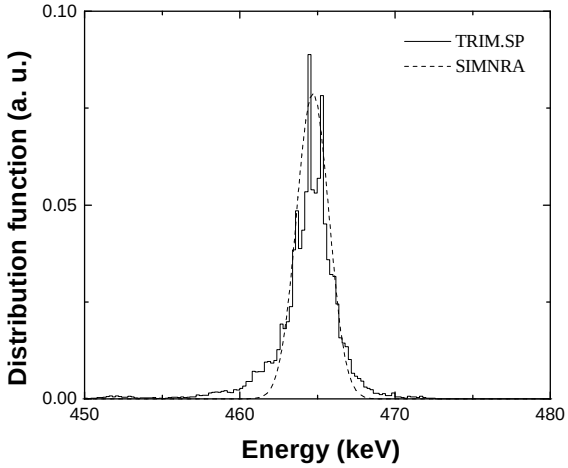

FIGURE 4. Energy distribution due to multiple small angle scattering of 500 keV ^{4}He in Au in a depth of 1.6×10^{17} atoms/cm^2. Incident angle $\alpha = 60°$.

Propagation of Straggling in Thick Layers

The energy dependence of the stopping power results in a non-stochastic broadening (or squeezing) of an energy-distributed beam. According to [21] the propagation of straggling can be calculated in the following way: If an ion beam with initial mean energy E_i and width ΔE_i penetrates a sublayer with thickness Δx, then the width ΔE_f after penetration of the sublayer is given by

$$\Delta E_f = \frac{S(E_f)}{S(E_i)}\,\Delta E_i \qquad (1)$$

with E_f the mean energy after the sublayer and $S(E_i)$, $S(E_f)$ the stopping powers at the entrance and exit of the sublayer, respectively. The stochastic effects have to be added to the non-stochastic broadening from Eq. 1.

As an example Fig. 3 shows the energy loss straggling of 2500 keV ^{4}He ions in silicon. The beam broadening and squeezing below the stopping power maximum are clearly visible.

Geometrical Straggling

The finite size of the incident beam and the width of the detector aperture result in a spread $\Delta\beta$ of the exit angle β for outgoing particles [22]. This angular spread leads to an energy spread of the particles at the target surface due to a spread $\Delta\theta$ of the scattering angle θ and different path lengths of the outgoing particles in the material. These two contributions to geometrical straggling are not independent of each other and are computed simultaneously.

PLURAL SCATTERING EFFECTS

Usually the trajectories of ingoing and outgoing particles are approximated by straight lines, which are connected at a single point where the reaction took place (single scattering approximation). However, in reality the particle trajectories are determined by a large number of scattering events with small deflection angles, and additional deflections with large deflection angles may occur [23, 24].

Small Angle Scattering

Angular spread due to multiple small angle scattering has been calculated by Sigmund and Winterbon [25] and has been recently reviewed in [21]. SIMNRA uses the same algorithms as presented in [21] for the calculation of multiple small angle scattering, but approximates the energy spread distributions by Gaussian functions. This underestimates the wings of the distributions. The energy distribution of 500 keV ^{4}He in Au is shown in Fig. 4 together with results of the Monte-Carlo code TRIM.SP [26], which takes all collisions into account. The widths of the curves agree well, however, the wings of the distribution are underestimated by SIMNRA.

Large Angle Scattering

Plural scattering with large deflection angles is, for example, responsible for the background below the low energy edge of high Z elements [23, 24]. SIMNRA calculates plural large angle scattering approximately by taking all trajectories with two scattering events into account (dual scattering) [24], which is very similar to

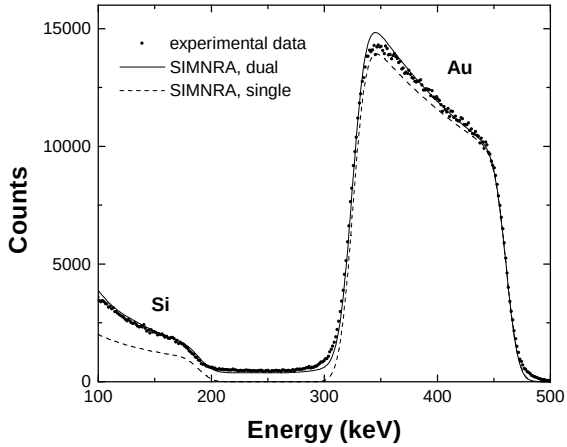

FIGURE 5. 500 keV ^{4}He backscattered from about 100 nm Au on Si, scattering angle $\theta = 165°$. Dots: experimental data; dashed line: SIMNRA with single scattering approximation; solid line: SIMNRA with dual scattering approximation.

the work of Weber *et al.* [27]. As an example the backscattering spectrum of 500 keV ^{4}He from Au on Si is shown in Fig. 5. With dual scattering a better agreement with the experimental data is obtained. The major drawback of dual scattering is the computing time, which increases by a factor of about 200 from several seconds to about 10 min on a Pentium 166 MHz processor.

ACKNOWLEDGMENTS

The TRIM.SP calculations were performed by W. Eckstein, whose help in all questions of plural scattering is gratefully acknowledged.

REFERENCES

[1] E. Kótai, Nucl. Instr. Meth. **B85**, 588 (1994).

[2] R. Doolittle, Nucl. Instr. Meth. **B9**, 344 (1985).

[3] M. Mayer, SIMNRA user's guide, Technical Report IPP 9/113, Max-Planck-Institut für Plasmaphysik, Garching, 1997.

[4] M. Mayer, *SIMNRA User's Guide, Version 4.4*, Part of the program package SIMNRA.

[5] J. Tesmer and M. Nastasi, editors, *Handbook of Modern Ion Beam Materials Analysis*, Materials Research Society, Pittsburgh, Pennsylvania, 1995.

[6] H. Andersen, F. Besenbacher, P. Loftager, and W. Möller, Phys. Rev. **A21**, 1891 (1980).

[7] M. Bozoian, Actual coulomb barriers, In Tesmer and Nastasi [5].

[8] L. Foster, G. Vizkelethy, M. Lee, J. Tesmer, and M. Nastasi, Particle-particle nuclear reaction cross sections, In Tesmer and Nastasi [5].

[9] R. Cox, J. Leavitt, and J. L.C. McIntyre, Non-Rutherford elastic backscattering cross sections, In Tesmer and Nastasi [5].

[10] G. Vizkelethy, Sigmabase: Data base and data server for ion beam analysis, http://ibaserver.physics.isu.edu/sigmabase/.

[11] J. Vorona, J. Olness, W. Haeberli, and H. Lewis, Phys. Rev. **116**, 1563 (1959).

[12] H. Andersen and J. Ziegler, *Hydrogen - Stopping Powers and Ranges in All Elements*, volume 3 of *The Stopping and Ranges of Ions in Matter*, Pergamon Press, New York, 1977.

[13] J. Ziegler, *Helium - Stopping Powers and Ranges in All Elements*, volume 4 of *The Stopping and Ranges of Ions in Matter*, Pergamon Press, New York, 1977.

[14] J. Ziegler, J. Biersack, and U. Littmark, *The Stopping and Range of Ions in Solids*, volume 1 of *The Stopping and Ranges of Ions in Matter*, Pergamon Press, New York, 1985.

[15] J. Ziegler and J. Manoyan, Nucl. Instr. Meth. **B35**, 215 (1988).

[16] W. Bragg and R. Kleeman, Philos. Mag. **10**, 318 (1905).

[17] M. Kumakhov and F. Komarov, *Energy Loss and Ion Ranges in Solids*, Gordon and Breach Science Publishers, New York, London, Paris, 1981.

[18] N. Bohr, Mat. Fys. Medd. Dan. Vid. Selsk. **18** (1948).

[19] J. Mayer and E. Rimini, *Ion Handbook for Material Analysis*, Academic Press, New York, San Francisco, London, 1977.

[20] W. Chu, Phys. Rev. **13**, 2057 (1976).

[21] E. Szilágy, F. Pászti, and G. Amsel, Nucl. Instr. Meth. **B100**, 103 (1995).

[22] D. Dieumegard, D. Dubreuil, and G. Amsel, Nucl. Instr. Meth. **166**, 431 (1979).

[23] P.Bauer, E. Steinbauer, and J. Biersack, Nucl. Instr. Meth. **B79**, 443 (1993).

[24] W. Eckstein and M. Mayer, Rutherford backscattering from layered structures beyond the single scattering model, presented at the COSIRES 98, submitted for publication.

[25] P. Sigmund and K. Winterbon, Nucl. Instr. Meth. **119**, 541 (1974).

[26] W. Eckstein, *Computer Simulation of Ion-Solid Interactions*, volume 10 of *Materials Science*, Springer, Berlin, Heidelberg, New York, 1991.

[27] A. Weber, H. Mommsen, W. Sarter, and A. Weller, Nucl. Instr. Meth. **198**, 527 (1982).